First lidar observations of mesospheric hydroxyl

E.J. Brinksma[1], Y.J. Meijer[1], 1.S. McDermid[2], R.P. Cageao[2], J.B. Bergwerff[3], D.P.J. Swart[3], W.A. Matthews[4], W. Hogervorst[1], J.W. Hovenier[1]

1. Vrije Universiteit, Faculty of Physics & Astronomy, Dc Boelelaan 10S 1, 10S 1 I IV Amsterdam, The Netherlands.

2. Jet Propulsion Laboratory, California Institute of Technology, Table Mountain Facility, Wright-wood, CA 92397, USA.

3. National Institute of Public Health and the Environment (RIVM), Air Research Laboratory, P.O. Box 1, 3720 BA Bilthoven, The Netherlands.

4. National Institute of Water and Atmospheric Research Ltd. (NIWA), Private Bag 50061, Omakau, Central Otago, New Zealand

For the first time, **ground-based lidars** have been **used to** identify **and detect** ground-state **(v"=0) hydroxyl** radicals (OH) in the **mesosphere** between -75 **and** S5 **km** altitude. These **lidars** operate near 308 nm **and** OH is **observed** through lnser-induced-fluorescence on **the** $A^2\Sigma^+-X^2\Pi$ (0,0) **band**. The results described h. *re* **potentially expose a valuable** global set of nighttime **OH observations, since existing long-term lidar data at several NDSC sites contain the (serendipitous) 011 informa-tion. Results** arc presented from **two mid-latitude** sites representing botb **the** northern and **south-ern hemispheres**, 'Table Mountain **(34°N)**, California, and Lauder **(45°S)**, **New Zealand**. They show **observations** of **a geometrically** thin (-3 km) **nocturnal layer** of **OH** near 80 km. A study of tbc **temporal behaviour** of the **mesospheric OH signal** following sunset, which supports previous model predictions 1 is **also** presented.

Hydroxyl radicals are the most reactive species in the atmosphere and play a pivotal role in atmospheric chemistry, but measurements of OH are difficult and sparse, Lidar measurements of OH in the mesosphere would be valuable, for example, to confirm model predictions and to track an important part of the mesospheric ozone and water budget., especially during noctilucent cloud events in the Arc-tic [D. Rees]. Nighttime lidar measurements could complement the few rocket-based or spaceborne measurements of groundstate 01 I in the high mesosphere which have been performed during day-time[2,3,4,5], as well as the observations of OH nightglow caused by transitions between high vibrational states (Meinel bands).

Several groups operating XeCl excimer laser based DIAL systems within the Network for the Detection of Stratospheric Change (NDSC), have observed pinks near 80 km in the 308 nm lidar return signals, These signals have been measured and archived routinely, for many years, for the purpose of ozone profiling, but until now the source or cause of these peaks had not been determined These peaks were observed during STOIC in 19S9 rrt TMF. Here, for the first time, we present substantial evidence that these peaks are caused by laser-induced-fluorescence (LIF) from mesospheric OH and can be used to detect ground-state OH in the mesosphere.

A typical observation, by the RIVM lidar[6] (Lauder, New Zealand, 45° S, 170° E), is shown in Fig. 1. The RIVM XeCl laser operates in a 'free running' mode, i.e., the laser light is emitted in a relatively broad spectrum centred at 30S nrn (emission linewidth typically 0.5 nm), which overlaps several OH absorption transitions within the OH $A^2\Sigma^+$-$X^2\Pi$ (0,0) band. Absorption in these lines gives rise to fluorescence on the (0,0) band resulting in enhanced return signals in the 30S nm spectral region, The observation that peaks only appear in the 30S run channel, and not in the 353 nm channel (Fig. 1) rules out scattering (by, e.g., mesospheric clouds) as the underlying process. At this altitude and pressure (-5. 10^{-3} mbar) collisional quenching of laser excited 011 $X^2\Pi$ is negligible and the radiative lifetime is on the order of 0.7 μs. Compared to the lidar resolution of 2 μs (equivalent to 300 m) this process causes minimal smearing of the altitude determination.

For the lauder site, the OH layer as observed is situated at 80 to S5 km altitude, and is geometrically thin (FWHM of about 3 km). This is in accordance with model calculations', which predicted that the nighttime OH number density profile should peak sharply at about SO km, at rnid-latitudes, clue to nighttime recombination at lower altitudes. Both the shape and the altitude of the observed feature differ from night to night, and frequently the feature is not observed or is below the detection limit

Other groups operating similar stratospheric ozone lidars within the NDSC were surveyed to determine the extent of observations. Those confirming observation of the OH feature include the JPL lidars at Mauna Lea, Hawaii and l'able Mountain, California; the GSFC mobile system, STROZ-LITE [McGee]; the ISTS lidars in Toronto and Eureka, Canada [Steinbrecht, Donovan]; the DWD lidar at Hohenpeissenberg, Germany [Steinbrecht], and the NILU lidar at ALOMAR, Andoya, Norway [Rees and Hansen]. A detailed study of the seasonal variation, as well as the differences between geographical locations, will be presented in a future article.

The experiments to try to prove that the lidar systems are indeed observing OH are presented below. They were performed using the JPL-TMF lidar at Table Mountain, California[7] but hold implications for all stratospheric ozone lidars. The JPL-TMF lidar usually operates in 'line-narrowed mode', where a tunable injection laser is used to seed and lock the wavelength of the amplifying laser. l-he resulting XCC1 laser output is tunable in the range from 307. S to 30S.3, although not continuously, and typically has a bandwidth of-8 pm.

The laser light was first directed through a propane flame, which is a source of OH, and the fluorescence intensity in a direction perpendicular to the laser beam was registered by a photomultiplier with a digital counter and an oscilloscope as a function of laser wavelength. This excitation spectrum thus provided a precise calibration of the laser wavelength and linewidth. The (merged) $P_1(1)/Q_{21}(3)$

doublet at 30S.16 run was partially resolved from the $Q_1(3)$ line at 30S. 15 nm confirming the line-\viJLh estimate of S pm.

The laser was then directed into the atmosphere, instead of through the laboratory 011 flame, and alternately tuned on and off the peak absorption using the laboratory experiment wavelength calibration. The results are presented in Fig. 2. Clearly, when the laser was tuned [o the wavelength of an OI I transition a peak was present in the lidar return and when it was tuned off it was not This strongly indicates that the observed peaks are caused by LIF from OH.

In Fig. 3, a series of consecutive measurements of the OI I feature, taken shortly after sunset, is presented. The experiment was performed using the JPL-TMF lidar, tuned to 308.1 nm. The temporal behaviour of the OH concentration in the first two hours after sunset is shown. The initial rise, the following decline, as well as the altitude shift of the OH peak concentration during the night all are in accord with model predictions'. Similar temporal behaviour has been observed at the TMF site during other nights in July and August of 1996, although the small initial rise in concentrations is not always present, Following these changes in the first ~2 hours after sunset the OI I signal reaches an essentially constant level, approximately 10°/0 of the peak shown in figure 3, and altitude which it maintains throughout the night. We have not observed any changes in the OH concentration or altitude distribution in the period immediately before sunrise.

Consideration of the OH number density and the corresponding absorption of the 308 nm laser radiation shows that this is extremely small and not useful for determining the 01 I concentration by the DIAL (differential absorption lidar) method. The possibility to use the I. It; signals to determine OH concentrations directly has been considered previously for tropospheric and stratospheric measurements (see for example McDermid et al.[8,9]). Unfortunately in the present experiments it would appear that we do not have sufficient information to allow us to derive the OI i concentration, although the magnitude of the observed signals is, presumably, directly proportional to the OI I density. There are uncertainties in the excited state energy redistribution, following laser excitation, and corresponding convolution of the emission spectrum with the lidar receiver spectral transmission. 'l'he fractional population of the specific ground-state level (X, v", J", K") excited by the laser compared to the overall OH population distribution is not known. These aspects of the problem arc further complicated since hydroxyl radicals are produced in this region of the atmosphere in ro-vibrational nonlocal thermodynamic equilibrium (NLTE) through the reaction of hydrogen atoms with ozone. Therefore, we cannot use the local temperature to calculate a Boltzmann distribution A kinetic model for state-to-state dynamics of 011 (v,J) in this region of the atmosphere has been developed by Dodd et al.[10] which clearly demonstrates the complexity of this system.

This model predicts that the nighttime OH ground-state number density, summed over all ro-rotational levels and spin sub-levels, is in the range of 10^4 to 10^5 molecules cm^{-3} for altitudes near SO km. Based on this model, we estimate that the ground-based lidar is capable of detecting the presence of

A new method to retrieve information about mesospheric 01 I from existing lidar signals has been presented. The first results show that a nocturnal layer of groundstate OI I is frequently observable in the high mesosphere at many sites around the world A series of consecutive lidar measurements, following sunset and throughout the night, shows the temporal behaviour of this layer which conforms with model predictions[1]. At present we are unable to quantify the number density of 01 I due primarily to the need for supplementary information concerning the NLTE population distribution of 01 I in the mesosphere and also concerning the rotational relaxation of the upper level following laser excitation. However, the current results do show quantitatively the nighttime behaviour of OI I (v''-O) which has not been observed before. Current research is continuing to attempt to quantify the OI I number density from the lidar measurements. In a future article, we will present a more extensive study of the geographical differences and the temporal behaviour of the nocturnal layer of ground-state OH, and a link between the lidar observations and atmospheric models

Bibliography:

1. Allen, M., J.I. Lunine, Y. L. Yung, The Vertical Distribution of Ozone in the Mesosphere and Lower Thermosphere, JGR, 89, D3, 4841 -4S72 (1984)

2. Anderson, J. G., Rocket-borne ultraviolet spectrometer measurement of OH resonance fluorescence with a diffusive transport model for mesospheric photochemistry, JGR, 76,4634-4652 (1971)

3. Anderson, J. G., Rocket measurement of OH in the mesosphere, JGR, 76, 7820-7824 (1971)

4. Morgan, M.F., D.G. Torr, M.R. Torr, Preliminary measurements of mesospheric 01 IX²II by ISO on Atlas 1, GM., 20, 6,511 -S14(1993)

5. Conway, R R., M.H. Stevens, J. G. Cardon, S.E. Zasadil, C.M. Brown, J.S. Morrill, G. II, Mount, Satellite measurements of hydroxyl in the mesosphere, GRL, 23, 16, 2093-2.096, (1996)

6. Swart, Daan P. J., Jan Spakman, Hans B. Bergwerff: RIVM's Stratospheric Ozone Lidar for NDSC Station Lauder: System Description and First Results. Abstracts of Papers of the 17th International Laser Radar Conference, Sendai, Japan, 405-408 (1994)

7. McDermid, 1. S., S.M. Godin and 1.,0. Lindquist, Applied Optics, 29, ?603 (1990)

8. McDermid, 1. S., J.B Laudenslager, and T.J. Pacala, The 1 Iydroxyl Radical: Verification of LIDAR Experiment, JPL Document D-493 (1983)

9. McDermid, 1. S., J.B. Laudenslager, and T.J. Pacala, New Technological developments for the remote detection of atmospheric hydroxyl radicals, Appl. Opt, 22, 2586-2591 (19S3)

10. Dodd, ./..4, S.J. Lipson, J.R. Lowell, P.S. Armstrong, W.A.M Blumberg, R.M. Nadile, S.M. Adler-Golden, W.J. Marinelli, K.W. Holtzclaw, and D. B. Green, Analysis of hydroxyl earthlimb emission: Kinetic model for state-to-state dynamics of OH, J. Geophys. Res., 99, 3559-3585 (1994)

Acknowledgements

EJB and YJM are indebted to Dr. S. Madronich, Dr. W. Ubachs and colleagues at NIWA Lauder, New Zealand for useful discussions. M. Schmoe, Dr. 1. Leblanc and K.F. Boersma are thanked for performing some of the measurements described. This work was carried out, in part, at the Jet Propulsion Laboratory, California Institute of Technology, under an agreement with the National Aeronautics and Space Administration

Correspondence *to* **E.J. Brinksma, ellen@nat.vu.nl**

Figure Captions

FIG 1 - Range corrected lidar return signals near 308 and 353 nm, as measured by the RIVM stratospheric lidar, Lauder, New Zealand, on March 10, 1997, at 9.30 PM local time. Note that the 308 nm signal peak is absent in the simultaneously measured 353 nm channel.

FIG 2 - Lidar return signals observed by the JPL-TMF lidar system, on August 9, 1996, showing that the OH feature is present in the 'ON' wavelength (bold lines, 308.1 nm) but absent in the 'OFF' wavelength (thin lines, 307.9 run). All measurements are integrated over 10 minutes, and are labelled with the time of observation Astronomical sunset was at 2:53 UT. For clarity, the signal-counts for the consecutive measurements have been successively offset by 400 counts.

FIG 3 - Consecutive lidar return signals observed on July 17, 1996, by the JPL-TMF lidar system. The observations were performed shortly after sunset, with an integration time of 28 minutes.

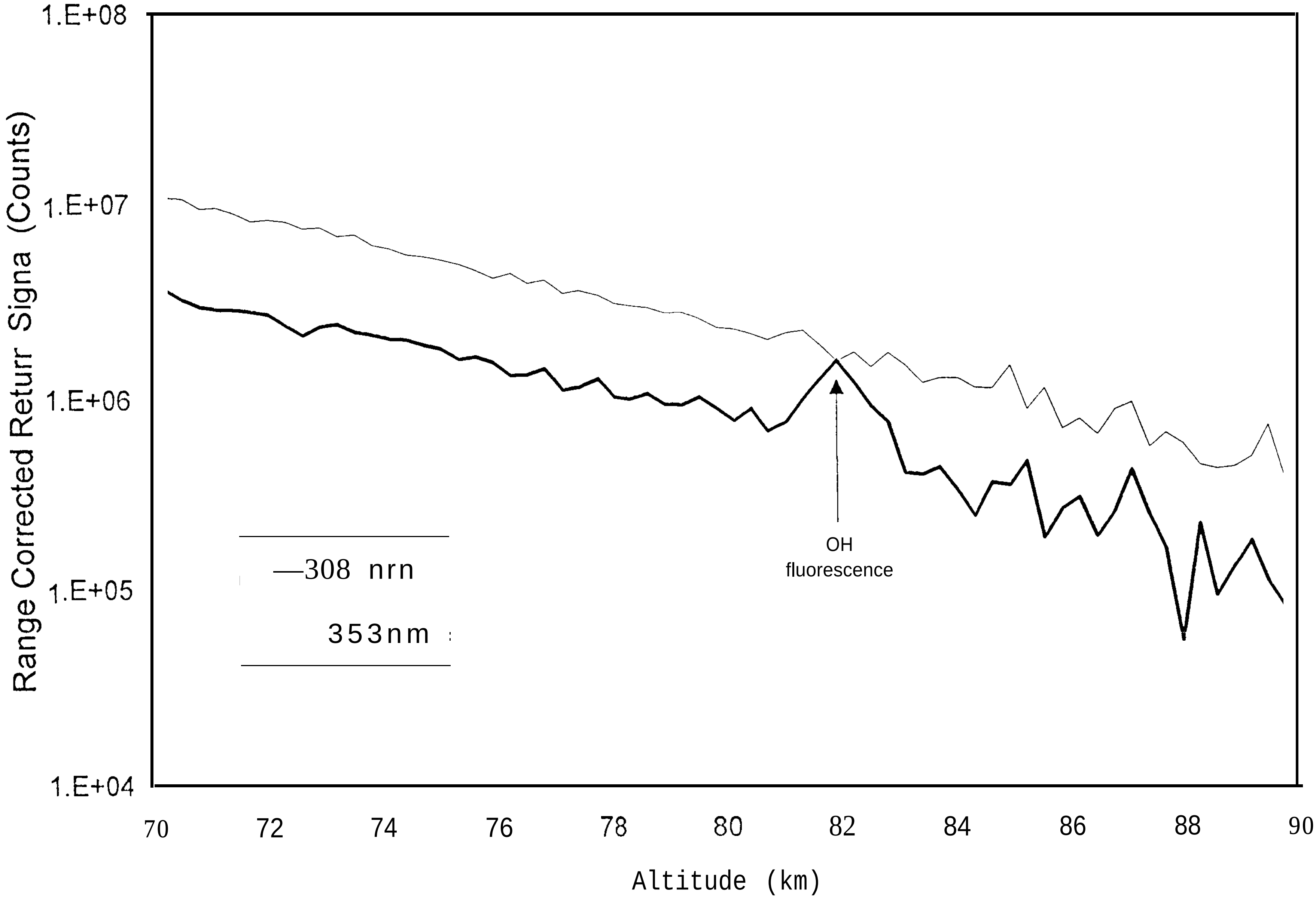
1.E+08
1.E+07
1.E+06
1.E+05
1.E+04
Range Corrected Returr Signa (Counts)
—308 nrn
353nm
OH
fluorescence
70
72
74
76
78
80
82
84
86
88
90
Altitude (km)

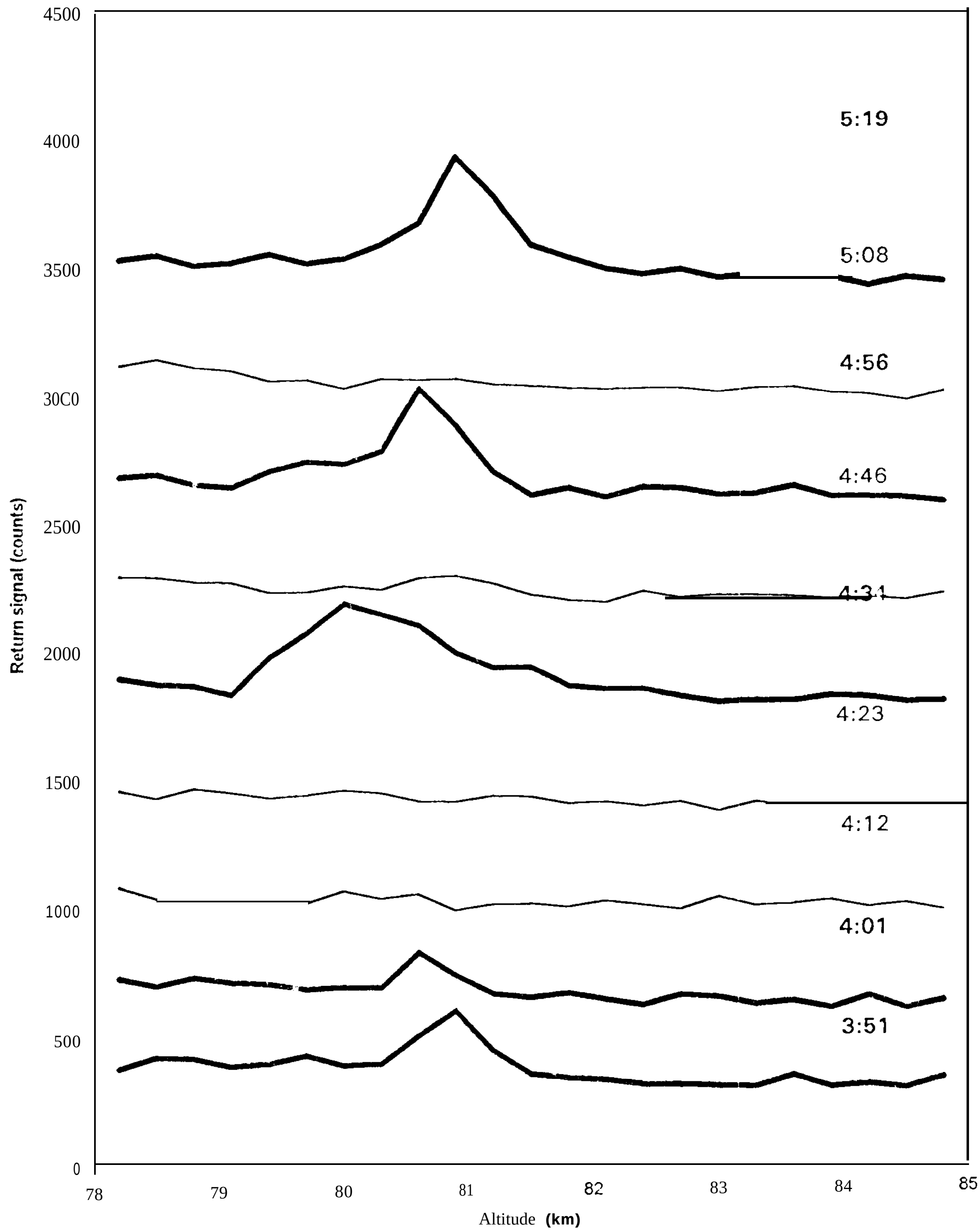

4500
4000
3500
30C0
2500
2000
1500
1000
500
0
Return signal (counts)
5:19
5:08
4:56
4:46
4:31
4:23
4:12
4:01
3:51
78
79
80
81
82
83
84
85
Altitude (km)

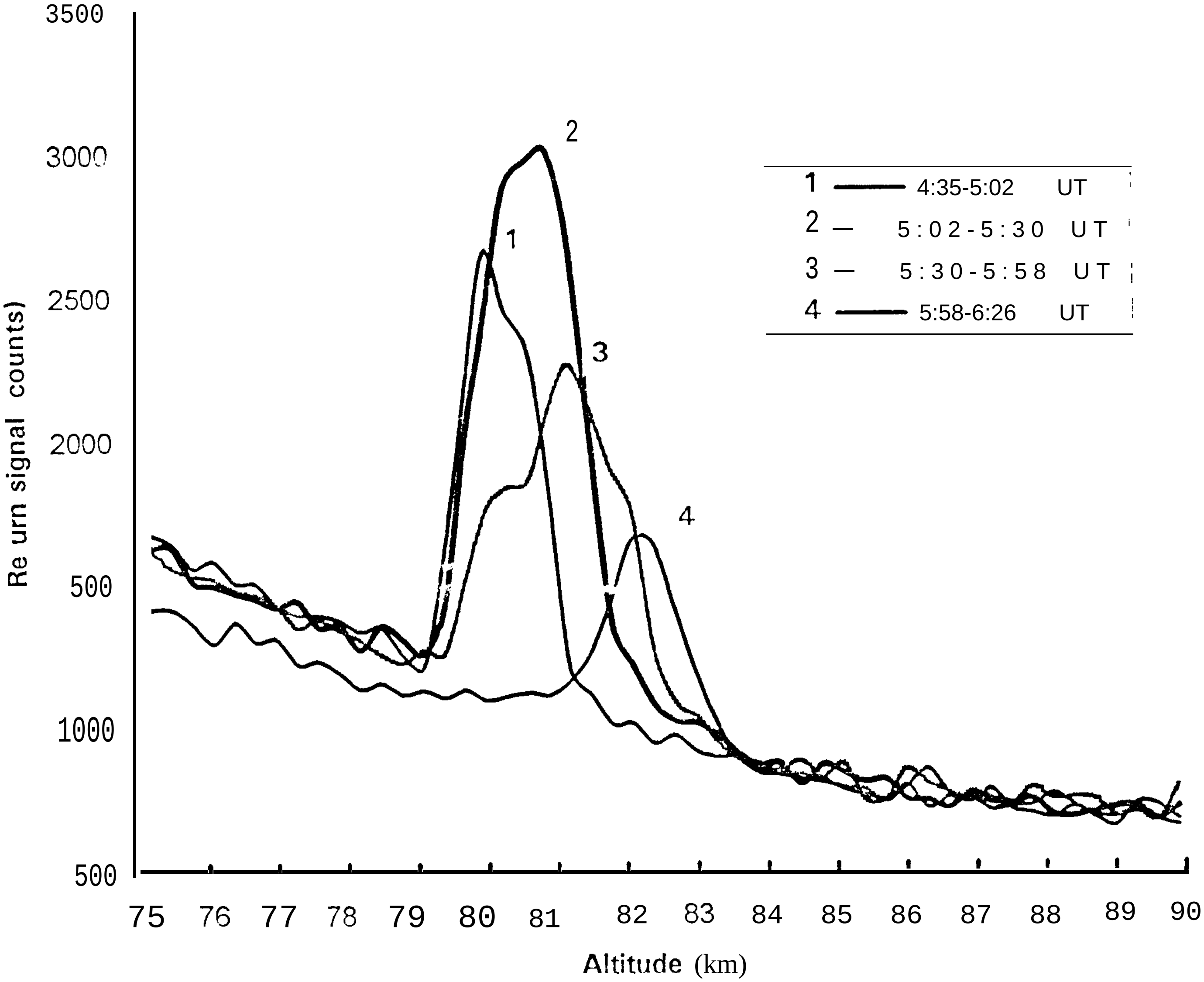

3500
3000
2500
2000
500
1000
500
Re urn signal counts)
1
2
3
4
1 4:35-5:02 UT
2 5:02-5:30 UT
3 5:30-5:58 UT
4 5:58-6:26 UT
75 76 77 78 79 80 81 82 83 84 85 86 87 88 89 90
Altitude (km)